ELSEVIER

International Journal of Fatigue 21 (1999) 485–495

International Journal of Fatigue

Long-term environmental fatigue of pultruded glass-fiber-reinforced composites under flexural loading

Kin Liao[a,*], Carl R. Schultheisz[b], and Donald L. Hunston[b]

[a]School of Applied Science, Division of Materials Engineering, Nanyang Technological University Nanyong 639798, Singapore

[b]Polymers Division, National Institute of Standards and Technology, Gaithersburg, MD 20899-0001, USA

Received 17 August 1998; received in revision form 12 October 1998: accepted 23 November 1998

Abstract

Pultruded glass-fiber-reinforced vinyl ester composite coupons were subjected to four-point-bend fatigue in various environments to study long-term durability for infrastructure applications. Several groups of specimens were aged in water or in salt solutions containing either 5 % mass fraction of NaCl or 10 % mass fraction of NaCl for up to 6570 h. Both as-received and aged specimens were then cyclically tested in air or while immersed in water or in salt solution. For specimens cyclically loaded at or above 45 % of the average flexural strength of the dry coupons, no substantial difference in fatigue life was observed among all the specimen groups. For samples cyclically loaded at 30 % of the dry flexural strength, however, all specimens tested in air survived beyond 10^7 cycles while all those tested in water environments did not. It is found that long-term environmental fatigue behavior is not controlled by the quantity of water absorbed; rather, it is governed by a combination of both load and fluid environment. No difference in fatigue life was found for specimens aged in different fluid environments at room temperature prior to fatigue testing. Relative to these samples, however, a significant difference was seen for specimens aged in water at 75 °C for 2400 h prior to cyclic test at load levels above 30 % of the dry flexural strength. When tested at 30 % of the dry flexural strength the differences were within the experiimental uncertainty. Microscopic examination of the fatigue specimens revealed evidence of a degraded fiber/matrix interphase region in those specimens where environmental exposure caused premature failure so this is believed to be a controlling factor in the environmental performance of the glass composite.

Key Words: *accelerated aging; bending fatigue; composites; fiber/matrix interphase; glass fiber; pultrusion; salt solution; vinyl ester; water*

1. Introduction

Glass-fiber-reinforced composites (or glass-fiber-reinforced plastics, GFRP) have seen limited use in the building and construction industry for decades [1-3]. Because of the need to repair and retrofit rapidly deteriorating infrastructure in recent years, the potential for using fiber-reinforced composites for a wider range of applications is now being realized [4-9]. These materials offer excellent resistance to environmental agents and fatigue as well as the advantages of high stiffness-to-weight and strength-to-weight ratios when compared to conventional construction materials. However, one of the obstacles preventing the extensive use of composites has been a lack of long-term durability and performance data. Although there have been numerous studies of fatigue and environmental fatigue with composite materials in the past three or four decades, most of those devoted to structural composites have focused on aerospace applications. Reviews on the fatigue behavior for composite materials can be found in Refs. 10-13.

At this time, the construction industry has focused predominantly on lower-cost glass reinforcement rather than the carbon fiber reinforcement used in aerospace applications. In addition, the expected service life is much longer in infrastructure applications. For instance, some bridges are designed to last for over 50 years. Hence the infrastructure community must be concerned with longer-term behavior as well as different materials and service environments than the aerospace industry. As a result, although data and experience gained from the past may serve as a general guideline, new studies and data pertaining to infrastructure applications are in great demand, especially for

*Corresponding author, Tel: +65-790-6258; fax: +65-792-6559, E-mail address: askliao@ntu.edu.sg (K. Liao)

composites produced by low-cost, large-volume processing methods such as pultrusion.

Previous studies have shown that exposure to water and other corrosive fluids such as acids will degrade the properties and shorten the fatigue life of GFRP. Environmental fatigue performance of GFRP is influenced by all its constituents, that is, the fiber, the matrix, and the fiber/matrix interphase region [14-25]. Some studies focusing on each of these components will be briefly reviewed below.

1.1. Fiber Effects

It is well understood that glass fibers degrade upon exposure to corrosive fluids under stress [26-29]. Metcalfe and Schmitz suggested that the underlying mechanisms of stress corrosion is driven by the exchange of alkali metal ions (Na^+ and K^+) in the glass and hydrogen ions (H^+) of the attacking fluid [28,29]. Schmitz and Metcalfe also proposed that the stress corrosion process consists of two stages: the incubation period, which extends over approximately 95 % of the life of the fiber, is controlled by interaction of water with the cations in the flaws to build up hydroxyl concentration (pH) to a critical level; a rapid corrosion period of the silica network follows the incubation period where the flaws propagate to reach a critical size under corrosion and stress, leading to failure [28, 29]. Vauthier, *et al.* have shown that more broken fibers were found in environmentally aged GFRP samples than those without aging, implying degraded fiber strength [30]. Sekine, *et al.* have also shown evidence of fiber degradation during environmental fatigue where elements from glass fibers were found in the fluid [22]. Recently, Liao, *et al.* have shown, by measuring fracture mirrors from the broken glass fibers in GFRP, that the strength of glass fibers was degraded upon environmental aging [31].

1.2. Matrix Effects

Formation of matrix cracks may have a critical role in environmental fatigue failure. Carswell and Roberts have conducted an investigation on the fatigue behavior of chopped glass fiber strand mat reinforced polyester carried out in air and several liquid media including water and acids [32]. Samples tested in air showed many matrix cracks prior to failure, while only a few cracks were found in samples tested in acid media, which implies that failure followed fairly quickly after the formation of first matrix crack in the acid media. Hofer, *et al.* also suggested that, in a study of glass/epoxy composites, moisture entering the network of matrix cracks rapidly affects the strength, elastic modulus, and strain capability of the fiber/matrix interface region of the plies immediately beyond the last cracked ply. This accelerates matrix cracking and shortens the overall life of the composite [33].

1.3. Interface Effects

The fiber/matrix interface region can have a controlling effect on the environmental fatigue of composites. Fiber/matrix debonding can be found during environmental aging even without externally applied loads [15]. When comparing the microscopic features of several types of GFRP fatigued in air and in water under tensile stress, Watanabe found that the failure surfaces of the samples in water were uneven, with much debonding [34]. The rate of reduction of fatigue strength in off-axis specimens in water was higher for unidirectional specimens, implying direct impact of water on the interphase region. Fried found significant degradation in shear fatigue strength after sea water exposure of GFRP up to five years, which strongly points to interface effects [35]. Moreover, it has been shown that surface finish on glass fibers leads to a significant difference in fatigue performance [36, 37].

Much effort in understanding the fatigue and environmental fatigue behavior of GFRP has been focused on tensile fatigue, with less attention being given to the fatigue behavior under other types of loading. Long-term data beyond 10^7 cycles is very limited for environmental fatigue of GFRP, especially in the case where the material is undergoing cyclic loading while immersed in fluid. In particular, long-term environmental fatigue data for pultruded GFRP under flexural loading is not well explored. As mentioned earlier, lack of long-term durability data is one of the technical obstacles preventing the extensive use of GFRP in construction. In light of this problem faced by the construction industry, the present work is concerned with generating long-term fatigue and environmental fatigue data for pultruded GFRP and developing an understanding of the performance-limiting issues so that confidence can be gained to use GFRP for applications in large scale primary and secondary structures.

2. Material and Method[1]

The material under study is pultruded E-glass fiber-reinforced vinyl ester composite provided by Strongwell, Bristol Division (formerly called Morrison Molded Fiber Glass, MMFG) and is designated EXTREN® 625. The as-received materials were 30.5 cm x 122 cm x 0.64 cm (12 in x 48 in x 0.25 in) plates. Bar specimens of dimensions 12.7 cm x 1.3 cm x 0.64 cm (5.0 in x 0.5 in x 0.25 in) were cut from the plates according to the ASTM standard (D790-92) for four-point bend test. Structurally, the material consists of unidirectional fiber roving and layers of chopped fiber strand mat embedded in vinyl ester matrix, shown schematically in Fig. 1. The fiber volume fraction determined by burn-off experiments is about 34 % with a standard uncertainty of 2 %. As a result of the pultrusion process, the fiber roving are not uniformly distributed locally.

[1]Certain commercial materials and equipment are identified in this paper in order to specify adequately the experimental procedure. In no case does such information imply endorsement by the National Institute of Standards and Technology, nor does it imply necessarily that the items are the best available for the purpose.

Also, because of the relatively small size of the test specimens (0.83 cm^2 cross sectional area), some specimens may contain more fiber roving than others, which gives rise to considerable data scattering in mechanical properties.

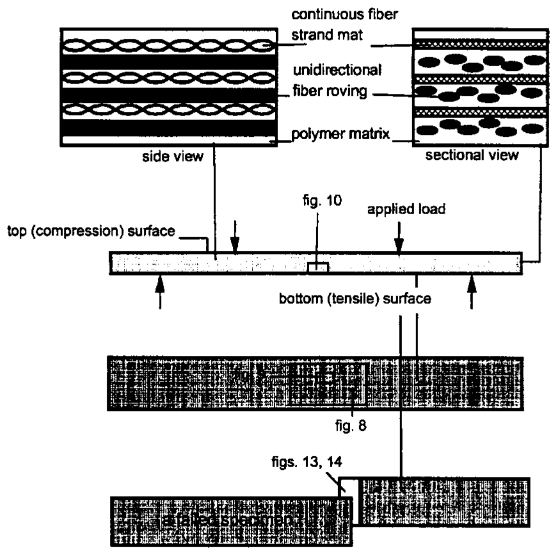

Figure 1: *Schematic of the structure of pultruded composite coupon under study. The locations of pictures that were taken form the specimens are also indicated.*

Some of the specimens were preconditioned by immersion in a fluid at room temperature or elevated an temperature for various times prior to testing in the same fluid at room temperature. The fluids were water or aqueous salt solution containing either 5 % mass fraction of NaCl or 10 % mass fraction of NaCl. The terms 5 % salt solution and 10 % salt solution will be used here to designate the appropriate salt solution. The four types of preconditioning are:

- **a.** de-ionized water for up to 3940 h at room temperature,
- **b.** 5 % salt solution for up to 4980 h at room temperature,
- **c.** 10 % salt solution for up to 6570 h at room temperature, and
- **d.** de-ionized water for up to 2400 h at 75 °C.

Water and salt solutions were chosen to simulate rain and salt spray, two commonly encountered outdoor environments. Mass changes for the specimens during preconditioning were recorded at regular time intervals using an electronic balance.

Four point bend loading, a very common loading situation in infrastructure, was chosen for this study. Quasi-static flexural strength and flexural modulus for as-received specimens as well as for preconditioned specimens were determined according to ASTM standard (D790-92) for the four point bend test.

Specimens were cyclically loaded using sinusoidal wave function at 10 Hz, with R=10 (where R is the ratio of the maximum to the minimum cyclic load) at room temperature in six different conditions:

- **A.** air (dry),
- **B.** room temperature water (specimens with no preconditioning),
- **C.** room temperature water (specimens preconditioned in water, condition **a**),
- **D.** 5 % salt solution (specimens preconditioned in 5 % salt solution, condition **b**),
- **E.** 10 % salt solution (specimens preconditioned in 10 % salt solution, condition **c**), and
- **F.** room temperature water (specimens preconditioned in hot water, condition **d**).

When testing under cyclic load, specimens were sealed in nylon bags filled with de-ionized water or salt solution. Cyclic tests were conducted at 4 different loadings. If the mean flexural strength for samples with no preconditioning tested in air at room temperature is designated FS, then the cyclic loading was adjusted so that the maximum load during the cycle was 85 %, 65 %, 45 %, or 30 % of FS. In the remainder of the paper, the terms 85 % FS, etc. will be used to designate the testing load that is utilized. Periodically, the tests were interrupted to measure the flexural modulus by means of a displacement gage (MTS® model 632.06H-20) and to record weight change of the specimen using an electronic balance. Surface related damage during fatigue was also observed using a microscope and recorded during these examinations. Because long-term loading is our primary concern, fatigue tests were *not* carried out at all the selected load intervals for each of the conditions (**A** through **F**). Only specimens from conditions **A** ,**B,** and **C** were tested at 85 % FS; specimens from conditions **A** through **D** were tested at 65 % and 45 % FS; and specimens from all of the conditions **A** through **E** were tested at 30 % FS. A test matrix is summarized in Table I.

3. Results and Discussion

3.1. Quasi-static flexural strength and modulus

The flexural modulus and quasi-static flexural strength for as-received specimens and those after preconditioning in conditions **a.** water , **b.** 5 % salt solution, **c.** 10 % salt solution, and **d.** 75 °C water, are shown in Figs. 2 and 3, respectively. Flexural strength, S_f, is determined as the maximum tensile stress on the lower outer surface according to ASTM Standard (D790-92):

$$S_f = P_c L/bd^2 \quad (1)$$

where P_c is the failure load, *L, b*, and *d* are the length, width, and thickness of the specimen, respectively. Note that FS is the average value of S_f for as-received specimens (no preconditioning) tested in air at room temperature. Compared to the as-received specimens, the flexural modulus for those after preconditioning remains essentially the same (Fig. 2). The quasi-static flexural strength after preconditioning, however, showed some degree of

Table 1: Test matrix

Pre-fatigue conditioning	Fatigue conditioning[a]	Quasi-static test	Fatigue load level (% FS)			
			30	45	65	85
-	A. air	8	3	5	5	5
-	B. water	-	5	4	3	3
a. 3940 h RT water	C. water	3	3	5	4	4
b. 4980 h RT 5 % NaCl	D. 5 % NaCl	3	3	3	3	-
c. 6570 h RT 10 % NaCl	E. 10 % NaCl	3 3	-	-	-	
d. 240 h RT 75 °C water	F. water	5	6	3	3	-

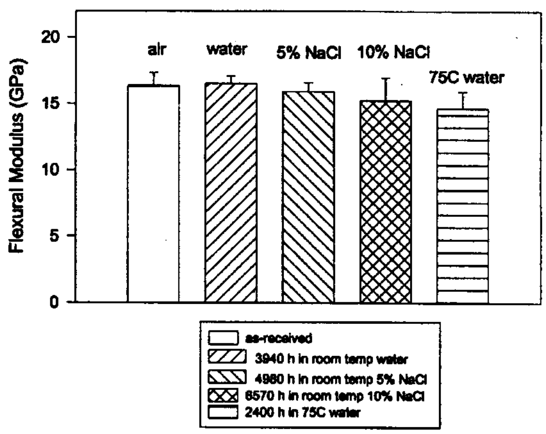

Figure 2: *Flexural modulus of pultruded composite coupons before and after environmental aging. Error bars represent the standard uncertainty in the experimental data, which is calculated as one standard deviation.*

degradation (Fig.3). The mean quasi-static flexural strength for specimens preconditioned in conditions **a**, **b**, **c,** and **d** showed decreases of 4.8 %, 12 %, 13 %, and 40 %, respectively, relative to that the samples not preconditioned. A t-test on the data using pooled variances indicated that the changes in strength for specimens aged under conditions **b, c,** and **d** are significantly different at a 95 % confidence level while the changes for specimens aged under condition **a** are significantly different at a 90 % confidence level. These data are in general agreement with data from previous studies on environmental aging of GFRP where degradation of tensile and flexural strength of GFRP after immersion in water and salt solution at room temperature was reported [14-25]. The strength degradation in the environmentally aged specimens was found to be related to degradation of three components: the glass fibers, the fiber/matrix interphase region, and the matrix [18, 31].

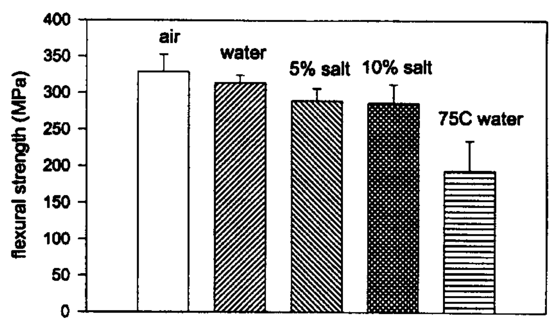

Figure 3: Flexural strength of pultruded composite coupons before and after environmental aging. Error bars represent the standard uncertainty in the experimental data. The legend is the same as Figure 2.

Macroscopic failure modes under mono-tonic flexural loading for the as-received specimens and specimens preconditioned at room temperature closely resemble each other. Typical load-displacement curves are shown in Fig. 4. These curves remains quite linear prior to failure. Note that the failure loads for the four specimens shown in Fig. 4 do not represent average values. The failure process under quasi-static loading begins with the development of parallel matrix cracks transverse to the longitudinal direction on the tensile surface (the lower surface sustaining tensile stress), followed by failure of the unidirectional fiber roving and propagation of longitudinal through-the-width cracks

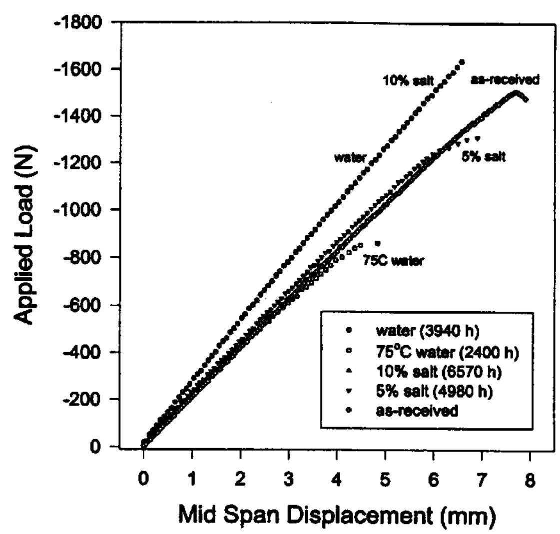

Figure 4: *Typical load versus mid-span displacement curves under four-point-bending. Data for the specimen labeled "water" are hidden behind the data labeled "10 % salt." The standard uncertainty in the experimental data is 5 N.*

between fiber roving and the layers of fiber strand mats, or between the fiber strand mats themselves. These large cracks are referred to as “delaminations” throughout the paper.

3.2. Sorption behavior

The amount of fluid absorbed by samples during preconditioning and cyclic loading was closely followed. Typical results are presented in Fig. 5, where the sorption data (percent mass change) for eight individual specimens are shown. All specimens shown in the figure had been loaded cyclically at 30 % FS. Each line in the Fig. 5 represents sorption data of one specimen. Hollow symbols represent sorption data taken from specimens under no externally applied load while filled symbols represent sorption data taken during cyclic loading (where the ordinate is time under cyclic load). For instance, the two lines connecting hollow circles represent sorption data from two individual specimens preconditioned in water, one for 4000 h, another for 5800 h. These specimens were then cyclically loaded to failure at 30 % FS, and their weight increase during cyclic loading was represented by filled circles. Similarly, squares and diamonds (hollow or filled) represent sorption data in 5 % salt solution and 10 % solution, respectively. Two specimens were cyclically tested at 30 % FS without preconditioning, sorption data during which period are represented by filled triangles.

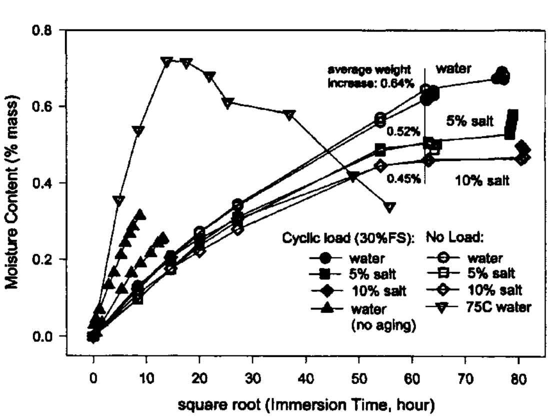

Figure 5: Sorption behavior of pultruded composite coupons under various aging conditions. The mass fraction of sorbed fluid is calculated as $(m-m_o)/m_o$, where m_o is the intial mass of the sample and m is the current mass. All the tests were carried out at 25 °C except those labeled “75C.” The relative standard uncertainty in the measurement of the mass fraction of sorbed fluid is estimated as 0.01 %.

Sorption behavior in three different fluids (i.e., water, 5 % salt solution, and 10 % salt solution) without externally applied load all seem to follow Fickian behavior (hollow symbols shown in Fig. 5): a rapid initial weight gain followed by saturation after prolonged immersion. Weight increase in the material depends on the type of media, concentration of the media, as well as externally applied load. For instance, average weight increase after 4000 h immersion in water, 5 % salt solution, and 10 % salt solution are 0.64 %, 0.52 %, and 0.45 %, respectively. It is also clear that the initial rate of weight increase is higher under cyclic loading. Compared to fluid weight gain during preconditioning, weight change during cyclic loading after preconditioning did not increase significantly in most cases. Rapid weight gain during fatigue after preconditioning was seen in only one or two cases, and may be attributed to large deformation or development of damage. It should be noted that the time for fluid sorption during cyclic loading at 30 % FS was less than 270 h for all specimens while the load-free time of immersion for most specimens was more than 5000 h. Weight increase during cyclic loading depends on load amplitude as well as time under load. For specimens tested under condition **B** where the specimens were not preconditioned before cyclically tested in water, the higher the cyclic load, the faster the initial sorption rate. The final increase in water content before failure, however, depends on the duration of the cyclic test, as shown in Fig. 6.

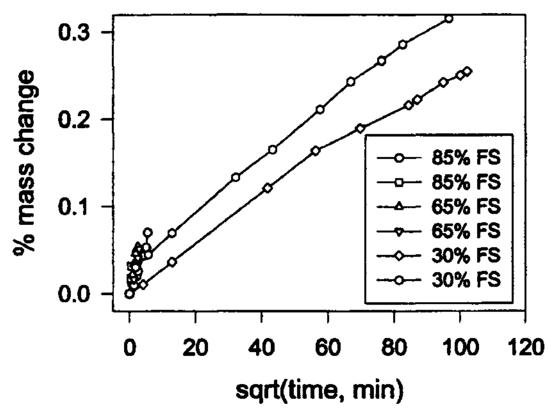

Figure 6: Sorption behavior of pultruded composite coupons under condition **B** *(cyclic loading in water without preconditioning). The relative standard uncertainty in the measurement of the mass fraction of water is estimated as 0.01 %.*

At 75 °C, the mass increase is much more rapid than at room temperature. Moreover, after reaching a maximum at about 200 h, the mass of the sample begins a steady decrease. This indicates that the water is abstracting material from the sample, a behavior that is not seen in any of the room temperature experiments. This is one indication that elevated temperatures may do more than simply accelerate the aging process.

How does sorption behavior influence fatigue life? Do the specimens behavior differently in water or salt solutions under cyclic load? These issues will be discussed in the subsequent section.

3.3. Fatigue Damage and Failure Mechanisms

Fatigue damage and failure mechanisms are accessed by both quantitative measurement of flexural modulus; and by macroscopic and microscopic observation of specimen surfaces during cyclic loading and after fracture. As has been well documented, change in elastic modulus is a strong indicator of the state of the material [11-13, 38]. Data collected from more than 30 individual specimens tested under conditions **A** through **F** suggests that degradation of flexural modulus is similar in generic pattern, independent of aging history, cyclic load levels, and environmental conditions. This similarity reflects a resemblance in the essence of damage development process. Some typical degradation curves are shown in Fig. 7, where flexural modulus and life (defined as cycles to failure) are presented in normalized scale. A flexural modulus degradation curve is typified by a small drop within the first 10 % of life, followed by a relatively flat region, indicating a slower rate of damage development, to about 80 % of life, then succeeded by a much faster drop during the last stages of life. Such a damage-related pattern of flexural modulus degradation is typical of fiber-reinforced composite materials [38]. Despite the gross similarity in the generic damage process, specific damage events may be load- or environment-dependent.

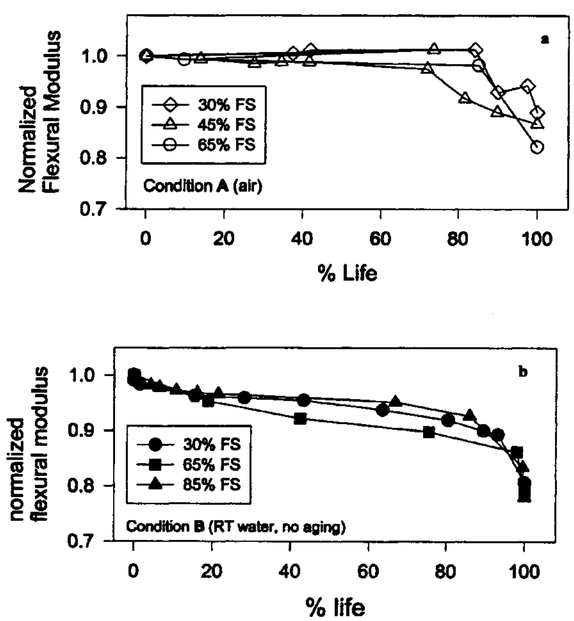

Figure 7: *Typical (normalized) stiffness degradation curves for specimens under cyclic loading under a) condition A (air), and b) condition B (room temperature water). The relative standard uncertainty in the normalized modulus data is estimated as 1.0 %.*

Transverse matrix cracks usually initiate from the edge of the specimen on the lower (tensile) surface, possibly as a result of micro-damage during specimen cutting. For specimens cyclically loaded above 45 % FS for all of the conditions **A**-**D** and **F**, visible transverse surface cracks can be found as early as 10 % of life while for those loaded at 30 % FS (conditions **A**-**F**) such cracks will not appear until mid- to late-life. Thus damage initiation is generally load-dependent and environment-independent at loading above 45 % FS. Cyclic loading at a level between 30 % FS and 45 % FS seems to be a demarcation for the initiation of environment-dependent fatigue damage. Small transverse cracks appear much earlier in conditions **B** through **F** (ranged from 43 % - 79 % of life) than those from condition **A** (90 % of life). Thus damage initiation is also environment-dependent at 30 % FS.

Damage development is generally load dependent. For specimens loaded at or above 45 % FS, more regularly spaced transverse surface cracks appear during mid-life (i.e., between 10-80 % of life). These cracks grow in length with an increase of applied load cycles, accompanied by a drop in flexural modulus (about 10 %) during early to mid-life. A typical transverse crack pattern on the surface of a specimen sustaining tensile load is shown in Fig. 8. Compared to specimens loaded at higher cyclic load levels, only a few transverse cracks were found throughout the life of those tested at 30 % FS. Debonding between longitudinally oriented fibers and matrix may occur as transverse matrix cracks advance (Fig. 9). By about 80-85 % of life, longitudinal cracks between layers of fiber strand mat or between fiber strand mat and unidirectional fiber roving begin to develop near the tensile surface. These interlaminar cracks grow quickly and develop into large delamination (Fig. 10), resulting in a significant drop in flexural modulus and leading to final failure. Delamination leading to final failure also occurs in specimens loaded at 30 % FS. Examination by scanning electronic microscope (SEM) reveals that fiber surfaces at the delamination are rather

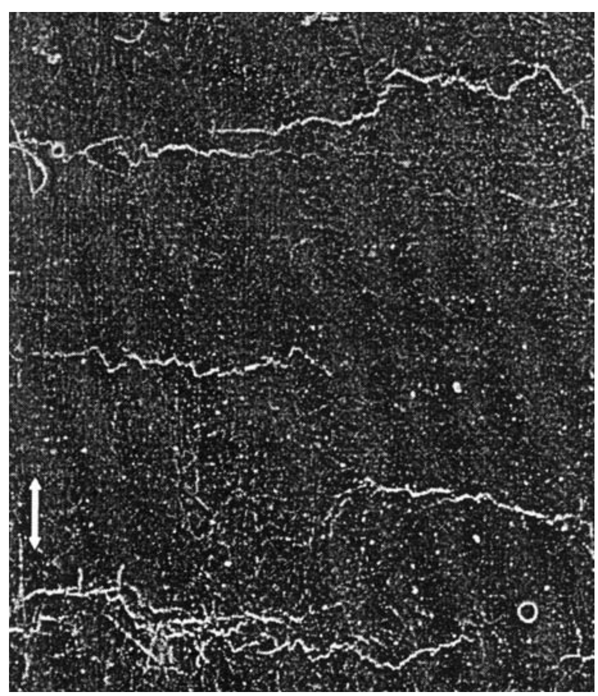

Figure 8: *Micrograph of typical transverse crack pattern of the bottom (tensile) surface of the specimen. The tensile laoding direction is indicated by the arrow, and the location of the view is shown in Fig. 1. The width of the image is 0.6 cm.*

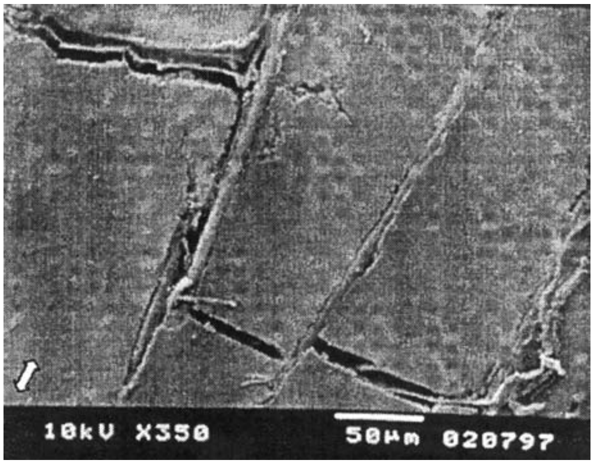

Figure 9: Scanning electron micrograph shows matrix cracks on the bottom (tensile) specimen surface transverse to the direction of tensile stress. Debonding between the matrix and the fibers can also be seen clearly. The tensile load direction is indicated by the arrow, and the location of the view is shown in Fig. 1.

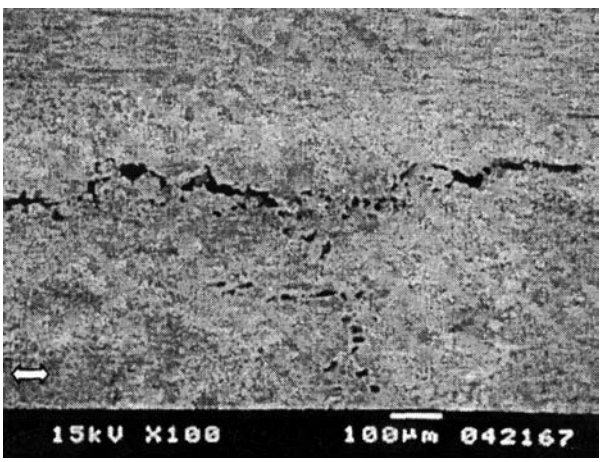

Figure 10: Scanning electron micrograph of crack associated with a delamination. The micrograph was taken from the edge of a specimen near the mid span. The bottom of the image is the tensile surface. The tensile load direction is indicated by the arrow, and the location of the view is shown in Fig. 1.

clean, suggesting a loss of adhesion between layers of fiber strand mat and between fiber strand mat and unidirectional roving. This facilitates growth of the delamination. Degradation curves for selected specimens tested in conditions **A** through **F** at 30 % FS are shown in Fig. 11. Judged by the much faster rate of decrease of flexural modulus for environmentally loaded specimens at 30 % FS (conditions **B**-**F**), damage development is environment-dependent at 30 % FS. In Fig. 11, the stiffness of two specimens tested under condition **A** showed a slight increase with applied cycles at mid-life. This increase is just outside the experimental uncertainty. If it is real, the change is unexpected, and there is no explanation at this point.

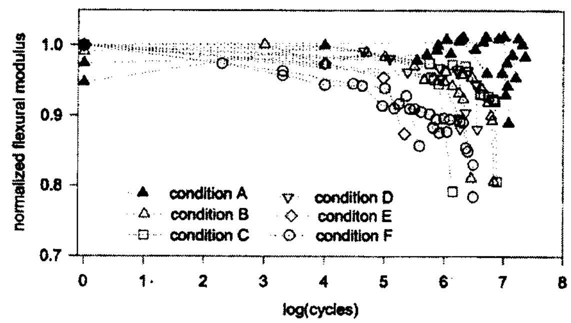

Figure 11: Degradation of flexural modulus during cyclic loading at room temperature for specimens under environmental condition **A** *through* **F**. *The relative standard uncertainty in the normalized modulus data is estimated as 1.0 %.*

3.4. SN Behavior

The SN data are presented in Fig. 12. The abscissa represents number of cycles to failure in the logarithmic scale while the ordinate represents maximum tensile stress on the specimen, σ, where $\sigma = P_m L/bd^2$; P_m is the maximum (peak) in the cyclic load while *L, b,* and *d* are the same as those in Eq. 1. The life data may be categorized into two regimes, a regime of stress-dependence and environment-independence, and a regime of stress- and environment- dependence. We shall first discuss the SN data for specimens tested after preconditioning at room temperature.

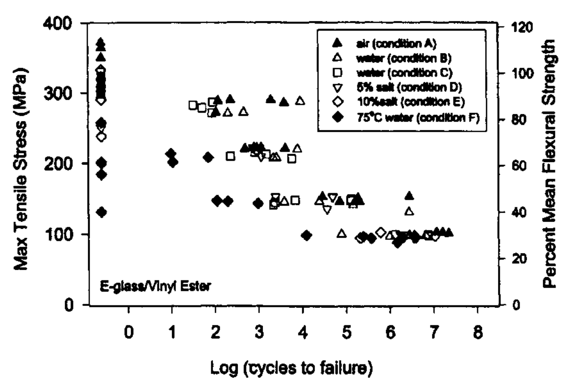

Figure 12: Stress-life (SN) data for pultruded composite coupons tested in fatigue at room temperature using environmental conditions **A** *through* **F**. *The standard uncertainty in the maximum applied stress is estimated to be 10 MPa.*

For specimens cyclically loaded above 45 % FS, it seems that the SN data are indistinguishable among conditions **A** through **D** (specimens from condition **E** were not above 30 % FS) as data points are overlapping. Although the quasi-static flexural strengths are decreased by preconditioning in water and salt solutions, no difference in fatigue life was found in the SN diagram. Of course, the experimental scatter was relatively large due to material variability so small differences in fatigue life might not be detectable. This regime of load-dependent and environment-independent fatigue behavior is characterized by high cyclic load levels and low cycles to failure (short loading time).

A significant difference in fatigue life starts to emerge for those samples tested at lower cyclic load levels. At 45 % FS, despite some overlapping of data for samples fatigued in dry and wet conditions, some of the dry specimens clearly survived to longer lives (number of cycles to failure). This loading appears to mark the transition between the two regimes. For specimens cyclically tested at 30 % FS, the dry specimens are clearly segregated from those tested under fluid environments. All dry specimens survived beyond 10^7 cycles while specimens tested under environmental conditions **B** through **E** all failed within 10^7 cycles. Most environmental SN data (i.e., specimens tested under conditions **B**, **C**, and **D**) loaded at 30 % FS are clustered within 10^6 to 10^7 cycles. The flexural moduli during fatigue start to show a decreasing trend at around 10^6 cycles. It is clear that water and salt solutions did exert a detrimental effect on the fatigue life during long-term experiments. This regime of load- and environment-dependence is characterized by low cyclic load levels and high cycles to failure (long loading time). A similar stress-life pattern has been reported by Phillips for stress-rupture of GFRP where he has suggested three distinct regimes, namely, environment-independent, environment- and stress-dependent, and stress-independent for the stress versus time-to-failure plot [39]. In our case, the existence of the first two regimes are apparent.

Although it has been shown by previous studies that fluids may exercise their corrosive effect on glass fibers to different extents depending on their pH value [29], this effect did not emerge from our fatigue data on composite coupons. This may be because the range of pH values covered here is small [40]. Much overlapping of data is seen on the SN plot for specimens tested under environmental conditions **B** through **E** between cyclic loads of 30 % to 65 % FS (Fig.12). Although aging in room temperature water results in some decrease in flexural strength, it seems that it has no significant influence on the fatigue life data when comparing those tested under conditions **B** (water, no preconditioning) and **C** (tested in water after preconditioning in water for 3940 h). In addition, the mass fraction of water absorbed does not seem to be a critical variable in fatigue life. For specimens tested under condition **C,** the mass fraction of water absorbed had almost reached saturation (about 0.7 %) before fatigue testing started while the mass fraction of water at fatigue failure was only about 0.3 % for samples tested under condition **B.** In fact, Bonniau and Bunsell have indicated that damage is not related to the quantity of water absorbed, but to the time of exposure and temperature after the water concentration limit was reached [16]. Comparing samples tested in condition **D** (5 % salt solution) and **E** (10 % salt solution) at 30 % FS level, the effect of salt concentration does not seem to have a significant role in fatigue life. In addition, a difference in life data between those tested in salt solutions and those tested in water is not found. As mentioned earlier, small differences may be difficult to detect since material variability caused the experimental scatter to be relatively large.

A fatigue limit has not been demonstrated from the data collected thus far. The fatigue behavior still depends on both environment and load at 30 % FS. If a regime exists where the behavior depends on environment but not load, it must be below 30 % FS. The concept that the matrix cracking stress in air may be taken as an allowable design stress [40] for environmental fatigue (as matrix cracking allows faster fluid ingress) is inconsistent with the data presented in this paper, because matrix cracking depends on both load and environment.

3.5. Fatigue Behavior After Accelerated Aging

Fatigue data for specimens tested under condition **F** (tested in room temperature water after aged in 75 °C water for 2400 h) are also presented in Fig. 12. In general, an accelerated effect in fatigue life is seen after aging in 75 °C water. Comparing the fatigue life data band of the hot-water aged specimens to those tested under conditions **A**-**E** at 65 % and 45 % FS, the former is at least a decade shorter than the latter. At a lower cyclic load (30 % FS), however, the difference seems to be diminishing, as most specimens tested under condition **F** survived to the 10^5-10^7 cycles range. Aging in water at elevated temperature has no doubt imparted damage to the fiber, matrix, and the fiber/matrix interphase region [31], its effect on fatigue behavior is more obvious at higher load levels while the stress-dependency is less pronounced at 30 % FS.

It has been suggested by a number of previous studies that the fiber/matrix interphase has a controlling effect in the environmental fatigue performance of fiber reinforced composites [33-37]. If the fiber/matrix interphase region is damaged or destroyed by fluid ingress, matrix cracks may propagate more easily because fibers have lost their reinforcing function. This process is also is further facilitated by the fact that the failure strain of the matrix (vinyl ester) is decreased upon aging in water [18]. In fact it was found that small matrix cracks appear earlier on the edge of specimens under environmental fatigue than those tested in air. Examination of the failure surfaces under SEM revealed a difference on the fiber surface. Typically, more matrix residue adhered to the fiber surface of specimens tested dry (Fig. 13), while "cleaner" fiber surfaces with much less matrix adhering are seen from specimens failed under environmental fatigue (Fig. 14). This difference on the fracture surface indicates that fluid action degrades the adhesion between the fibers and the matrix. The same observation is also reported by Wanatabe [34] and Sekine, *et al.* [23].

The process of environmental fatigue, then, involves coupled interaction between interphase degradation and matrix cracking: once cracks in the matrix are developed,

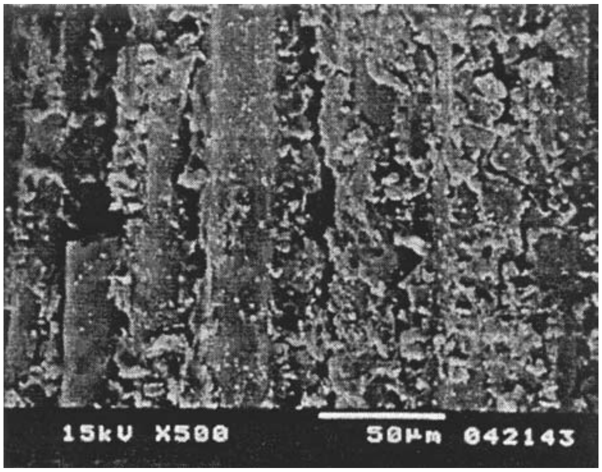

Figure 13: *Scanning electron micrograph of delamination surface for specimen failed by cyclic testing in air. The location of this surface is shown in Fig. 1.*

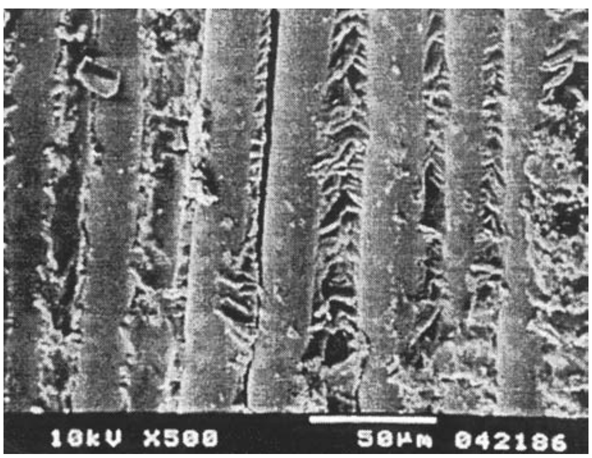

Figure 14: *Scanning electron micrograph of delamination surface for specimen failed in environmental fatigue. The location of this surface is shown in Fig. 1.*

ingress of corrosive fluid into the material is at a much faster rate, which further accelerates the degradation process of the interphase region. This coupled process exposes the glass fibers to corrosion at an increasing rate. Although degradation of fiber strength cannot be deduced from the fatigue data, strong evidence of fiber strength degradation during stress-free aging were well established from microscope studies of the failed samples.

4. Concluding Remarks

Based on the findings in this study, the following can be concluded:

- Aging in water and salt solutions at room temperature for up to 6570 h results in no significant drop in flexural modulus but a 5 % to 13 % degradation of flexural strength for the pultruded glass fiber reinforced composite. Aging in 75 °C water for 2400 h results in a modulus decrease that is not outside the experimental uncertainty but a 40 % degradation in strength.
- At cyclic loads above 45 % FS, specimens gave the same behavior when tested in air, in water, or in salt solutions. In this loading regime, the behavior depends on load but is independent of environment. The fatigue lives were less than 10^6 cycles in all cases.
- At a cyclic load of 30 % FS, however, results indicate that water and salt solutions have a significant detrimental effect on the life of the coupons (a regime of stress and environment-dependence). This regime is characterized with fatigue life beyond 10^7 cycles for dry coupons and within 10^7 cycles for those tested in a water environment.
- The data collected so far indicate that the fatigue lives of specimens preconditioned in water or salt solution for up to 6570 h did not appear to differ from those for specimens that were not preconditioned.
- Aging in 75 °C water for 2400 h did decrease the fatigue life; however, this effect is load-dependent. The effect is more obvious at 45 % FS and 65 % FS than at 30 % FS.
- Effect of fiber/matrix interfacial damage on fatigue performance is evident.

Acknowledgments

The authors thank Mr. Daniel Witcher of Strongwell, Bristol Division (formerly Morrison Molded Fiberglass) for the donation of pultruded GFRP plates.

References

1. Chambers, R. E., "Structural Fiber Glass-Reinforced Plastics for Building Applications," *Plastics in Buildings*, I. Skeist Ed., Reinhold Publishing Co., New York, 1965, pp. 72-118.
2. Hollaway, L., *Glass Reinforced Plastics in Construction,* John Wiley & Sons, New York, 1978.
3. Green, A. "Glass-Fiber-Reinforced Composites in Building Construction," *Transportation Research Record 1118*, Transportation Research Board, Washington, DC, 1987, pp. 73-76.
4. Barbero, E. and GangaRao, H. V. S., "Structural Applications of Composites in Infrastructure, Part I," *SAMPE Journal*, Vol. 27, No. 6, November/December 1991, pp. 9-16.
5. Barbero, E. and GangaRao, H. V. S., "Structural Applications of Composites in infrastructure, Part II," *SAMPE Journal*, Vol. 28, No. 1, January/February 1992, pp. 9-16.
6. *Advanced Composite Materials in Civil Engineering Structures*, S. L. Iyer and R. Sen Eds., American Society of Civil Engineers, New York, 1991.
7. *Infrastructure: New Materials and Methods of Repair, Proceedings of the Third Materials Engineering Conference*, K. D. Basham Ed., San Diego, California, November 13-16, 1994.
8. *Fiber Composites in Infrastructure, Proceedings of the*

First International Conference on Composites in Infrastructure (ICCI'96), H. Saadatmanesh and M. R. Ehsani Eds., Tucson, Arizona, January 5-7, 1996.

9. *High-Performance Construction Materials and Systems: An Essential Program for America and Its Infrastructure*, Executive Report 93-5011.E, The Civil Engineering Research Foundations, April, 1993.
10. Harris, B., "Fatigue and Accumulation of Damage in Reinforced Plastics," *Composites*, October, 1977, pp. 214-220.
11. Stinchcomb, W. W. and Reifsnider, K. L., "Fatigue Damage Mechanisms in Composite Materials: A Review," *Fatigue Mechanisms, ASTM STP 675*, American Society for Testing and Materials, 1979, pp. 762-787.
12. Agarwal, B. D. and l. J. Broutman, in *Analysis and Performance of Fiber Composites*, John Wiley & Sons, New York, 1980.
13. Konur, O. and Matthews, F. L., "Effect of the Properties of the Constituents on the Fatigue Performance of Composites: a Review," *Composites*, Vol. 20, No. 4, July, 1989, pp. 317-328.
14. Romanenkov, I. G., "Dependence of the Mechanical Properties of GRPs on their water Absorption," *Soviet Plastics*, Vol. 2, 1967, pp. 74-75.
15. Pritchard, G. and Taneja, N., "Water Damage in Polyester/Glass Laminates, Part II: Microscopic Evidence," *Composites*, Vol. 4, No. 4, 1973.
16. Bonniau, P. and Bunsell, A. R., "Water Absorption by Glass Fibre Reinforced Epoxy Resin," *Composite Structures*, I. H. Marshall Ed., 1981, pp. 92-105.
17. Martin, J. R. and Gardneer, R. J., "Effect of Long Term Humid Aging on Plastics," Polymer Engineering and Science, Vol. 21, No. 9, June, 1981, pp. 557-565.
18. Apicella, A. Migliaresi, C., Nicodemo, L., Nicolais, L., Iaccarino, L., and Roccotelli, S., "Water Sorption and Mechanical Properties of a Glass-Reinforced Polyester Resin," *Composites*, October, 1982, pp. 406-410.
19. Garg, A. C. and Pawar, S. K., "Environmental Effect on Fracture of Glass Fibre Reinforced Polyester," *Fibre Science and Technology*, Vol. 17, 1982, pp. 133-139.
20. Garg, A. C. and Paliwal, V., "Effect of Water on the Fracture Behavior of Glass Fibre Reinforced Polyester," *Fibre Science and Technology*, Vol. 17, 1982, pp. 63-69.
21. Rege, S. K. and Lakkad, S. C., "Effect of Salt Water on Mechanical Properties of Fibre Reinforced Plastics," *Fibre Science and Technology*, Vol. 19, 1983, pp. 31-324.
22. Komai, K., Minoshima, K., and Shiroshita, S., "Hygrothermal Degradation and Fracture Process of Advanced Fibre-Reinforced Plastics," *Materials Science and Engineering*, A143, 1991, pp. 155-166.
23. Sekine, H., Shimomura, K., and Hamana,N., "Strength Deterioration and Degradation Mechanism of Glass Chopped Reinforced Plastics in Water Environment," *ISME International Journal*, Series I, Vol. 31, No. 3, 1988, pp. 619-626.
24. Bradley, W., Chiou, P. B., and Grant, T., "The Effect of Seawater on Polymeric Composite Materials," *Composite Materials for Offshore Operations: Proceedings of the First International Workshop*, NIST Special Publication 887, S. S. Wang and D. W. Fitting, Eds., National Institute of Standards and Technology, August, 1995, pp. 193-202.
25. Grami, M., Moilanen, M. J., and Rosenow, M. W. K., "Environmental Degradation of Glass Fibers in Polyurethane Matrix Composites," *Proceeding of ICCM-10* Vol. VI, Whistler, B.C., Canada, August, 1995.
26. Charles, R. J., "Static Fatigue of Glass. I," *Journal of Applied Physics*, Vol. 29, No. 11, November, 1958, pp. 1549-1553.
27. Charles, R. J., "Static Fatigue of Glass. II," *Journal of Applied Physics*, Vol. 29, No. 11, November, 1958, pp. 1554-1560.
28. Schmitz, G. K. and Metcalfe, A. G., "Stress Corrosion of E-Glass Fibers," *I&EC Product Research and Development*, Vol. 5, No. 1, March, 1966, pp. 1-8.
29. Metcalfe, A. G. and Schmitz, G. K., "Mechanism of Stress Corrosion in E-Glass Filaments," *Glass Technology*, Vol. 13, No. 1, February, 1972, pp. 5-16.
30. Vauthier, E., Chateauminois, A., and Bailliez, T., "Hygrothermal Aging and Durability of Unidirectional Glass-Epoxy Composites," *Proceedings of the 10th International Conference of Composite Materials, Vol. VI*, August, 1995, pp. 185-192.
31. Liao, K., Schultheisz, C. R., and D. L. Hunston, "Effects of Environmental Aging on the Properties of Pultruded GFRP," submitted, *Composites*.
32. Carswell, W. S. and Roberts, R. C., "Environmental Fatigue Stress Failure Mechanism for Glass Fibre Mat Reinforced Polyester," *Composites*, April, 1980, pp. 95-99.
33. Hofer, K. E., Skaper, G. N., and Bennett, L. C., "Effect of Moisture on Fatigue and Residual Strength Losses for Various Composites," *Journal of Reinforced Plastics and Composites*, Vol. 6, January 1987, pp. 53-65.
34. Watanabe, M., "Effect of Water Environment on Fatigue Behavior of Fiberglass Reinforced Plastics," *Composite Materials: Testing and Design (Fifth Conference), ASTM STP 674*, S. W. Tsai, Ed., American Society for Testing and Materials, 1979, pp. 345-367.
35. Fried, N., "Degradation of Composite Materials: The Effect of Water on Glass-Reinforced Plastics," *Mechanics of Composite Materials, Proceedings of the Fifth Symposium on Naval Structural Mechanics*, F. W. Wendt, H. Liebowitz, and N. Perrone Eds., 1967, pp. 813-837.
36. Hofer, K. E., Jr., Benett, L. C., and Stander, M., "Effect of Various Fiber Surface Treatments on the Fatigue Behavior of Glass Fabric Composites in High Humidity Environment," *Proceeding of the 31st Annual Technical Conference of SPI*, Washington, D. C., February, 1976, Section 6-A.
37. Shih, G. C. and Ebert, L. J., "The Effect of the Fiber/Matrix Interface on the Flexural Fatigue Performance of Unidirectional Fiberglass Composites,"

Composites Science and Technology, Vol. 28, 1987, pp. 147-161.

38. Reifsnider, K. L., Schulte, K., and Duke, J. C., Jr., "Long-Term Fatigue Behavior of Composite Materials," *Long-Term Behavior of Composites, ASTM STP 813*, T. K. O'Brien Ed., American Society for Testing and Materials, Philadelphia, 1983, pp. 136-159.
39. Philips, M. G., "Prediction of Long-Term Stress-Rupture Life for Glass Fiber-Reinforced Composites in Air and Aqueous Environments," *Composites*, July, 1983, pp. 271-275.
40. Liao, K., Schultheisz, C. R., Hunston, D. L., and Brinson, L. C., "Environmental Fatigue of Pultruded Glass-Fiber-Reinforced Composites," *Composite Materials: Fatigue and Fracture, Seventh Symposium, ASTM STP 1330*, R. B. Bucinell, Ed. American Society for Testing and Materials, Philadelphia, 1998, pp. 217-234.